Net Magnetic Force Generation in Discontinuous Circuits: A Force Symmetry-Breaking Phenomenon

A Mohammadpour

Net Magnetic Force Generation in Discontinuous Circuits: A Force Symmetry-Breaking Phenomenon

A.Mohammadpour*

Imperial College of London, London, SW7 2AZ, United Kingdom

February-March 2024

Abstract

This paper explores the potential for generating a net magnetic force in circuits with open sections, where the asymmetry of interacting forces can produce a resultant force. A general proof is given, and it is shown that the Lorentz magnetic force between two wires can be decomposed into reciprocal and directional components. Reciprocal components generally produce no net force, while directional forces vanish in closed circuits but may remain nonzero in discontinuous circuits. Additionally, it is demonstrated that asymmetries in the field and self-induced stress tensors can behave similarly to external forces, causing a change in total momentum. Both radiative and non-radiative forces are obtained, and it is shown that when radiation is negligible, non-radiative force prevails. The central concept behind this work stems from a nuanced idea that may have been overlooked or remained unnoticed. The proposed idea's simplicity could lead to the development of affordable propellant-less(non-chemical)[1] propulsion systems for space applications, such as the repositioning of satellites.

1 Introduction

This paper explores an intriguing thought experiment. Before delving into the specifics, let's consider the famous example of two point charges moving perpendicular to each other, both approaching a common origin at a distance far from it [1, 2]. Due to the Lorentz force and Biot-Savart law, these point charges will experience equal magnetic forces perpendicular to their moving path in distinct directions, seemingly violating Newton's third law. Regarding this violation, Feynman, in his lecture notes, volume II, chapter 27 [2], states that the field

*Corresponding author. Email: A.mohammadpourshoorbakhlou@imperial.ac.uk

[1]No mass is expelled thus propellantless in the traditional sense.

momentum balances the change of the particle momenta. He has suggested that as long as the overall balance of momentum is maintained, the violation of the third law should be less concerning, and he leaves the reader to decide the generality of Newton's third law.

Now, imagine two wire loops carrying currents. If we neglect the retardation effect[3], Newton's third law mandates that they must exert equal and opposite forces on each other. Can we design the loops' geometry and orientation to create a scenario similar to the point charge experiment, where interaction forces act in different directions without canceling each other?

A strict physicist might immediately assert that this is impossible. Indeed, the mathematics presented in the Methods section proves that any two closed loops exert equal and opposite forces, resulting in overall cancellation. However, a question immediately arises: if two closed loops must produce equal and opposite forces, does removing part of a loop break this symmetry? As we will subsequently see, discontinuous circuits[2] can indeed exhibit this force symmetry breaking.

In the study by Mohammadpour [3], it is argued that Newton's Third Law is only locally applicable at the point of interaction between fields and charges, where an instantaneous exchange of momentum occurs. It is deemed inappropriate to extend Newton's Third Law to interactions at a distance where retardation effects may occur and the state of the charges may change. Sebens [5] discusses since fields exert forces on charges and, conversely, charges exert forces on fields, Newton's Third Law is preserved. Considering the locality of Newton's Third Law and using the Lorentz force as defined in equations (6) and (7), we can demonstrate that forces acting on two open wires might not always exhibit symmetry(Please refer to section Methods).

The accuracy of calculated forces using the Lorentz force is difficult to dispute. This is because the Lorentz force is deducible from Faraday's law of induction and Maxwell's equations using the Leibniz integral rule (A detailed proof is in [6, 7, 8]). Since Maxwell's equations offer an accurate description of fields for most classical electromagnetic applications, it's reasonable to consider the Lorentz force equally accurate when representing forces within the mentioned domain of application.

Numerous concepts have been proposed that utilize electromagnetic principles for space travel. However, few of them have solid experimental or theoretical evidence. One of these exciting proposals exploit retardation and phase difference concepts for net force generation [9, 10]. The feasibility and criticisms of such propulsion systems are discussed in [11, 12][3]. Despite their potential,

[2]The circuit is called discontinuous in the sense that conductors are omitted, but the electromagnetic fields are continuous. The displacement current ensures the continuity of the current and fields as the first time suggested by J.C. Maxwell [4].

[3]These critiques are not themselves devoid of criticism. For instance, [11] assumes that the force calculated on the wires is similar to that on "point" dipoles and that the produced force results from the radiation momentum. Consequently, it is concluded that the energy expenditure to momentum gain ratio is light speed C. This assumption is only valid if we disregard the non-radiative part of the fields and exclude the non-zero effect of Maxwell's stress tensors in the momentum equation.

thrust generation through retardation typically demands high frequencies or rapid current/charge changes. This often results in substantial inductive reactance in the circuits, posing a significant engineering challenge due to the necessity of high voltages[4]. Furthermore, radiative power losses increase notably with frequency, negatively impacting the thrust-to-power ratio. Despite these challenges, retardation-based force generation has been suggested to be used for testing the anisotropy of the one-way speed of light [3][5].

The EM drive has also undergone various experiments [13, 14]. However, regardless of the feasibility of such a thruster, the theoretical background has not yet been established to aid in accurate design.

Other types of electromagnetic engines like Plasma and Hall thrusters utilize ionized gas propellant [15, 16, 17, 18]. These are gaining traction for deep space missions due to their efficiency in comparison to chemical rocket engines [19]. However, their propellant requirement limits their range for extended journeys. Additionally, at the current stage of development, the forces produced are tiny, which limits their broader application.

Recently, a propellant-less propulsion concept based on asymmetrical electrostatic pressure has been introduced [20][6]. It is claimed that the magnitude of thrust is geometry-dependent in the proposed propulsion system, potentially limiting its design and flexibility.

The concepts presented in this paper rely on symmetry breaking. Unlike [20], symmetry breaking of magnetic forces is utilized here. Magnetic fields can store more energy per unit volume than electric fields, making them attractive for converting electrical energy to mechanical energy, as seen in electric motors. Unlike electric fields prone to material breakdown, magnetic fields can be intensified without similar risks, especially within solid materials like metal cores. Furthermore, the force generated in this work can be enhanced through both geometric optimization and current increase, achievable via techniques like winding wires, increasing open sections, and utilizing superconductors.

In this paper, in Section 2, the theoretical aspects are discussed, illustrating the non-reciprocity of forces in discontinuous circuits. It is also shown that asymmetries in stress tensors can lead to changes in total linear momentum. In Section 3, a simple circuit setup is exemplified, demonstrating that significant forces can be generated, highlighting the potential for practical aerospace applications.

[4]Although we can reduce inductive reactance using an LC setup, technically, it remains challenging to maintain high current and high frequency.

[5]Note that the constancy and isotropy of the two-way speed of light may not inherently imply the same for the one-way speed of light.

[6]The theoretical aspects of this proposal are not explained fully; however, the patent report experimental observations claiming net force generation.

2 Methods

2.1 General proof of non-reciprocal forces in discontinuous circuits

In the electrodynamic causality context, the magnetic field's exact solution around the wire from the Maxwell equation is presented in [21]. However, when neglecting the retardation effect and radiation terms by assuming a low rate of change in current, this description simplifies to the more familiar Biot-Savart law [7] [1]

$$\mathbf{B} = \frac{\mu_0 I}{4\pi} \oint \left(\frac{d\mathbf{l}^s \times \mathbf{r}}{r^3} \right) \tag{1}$$

where μ_0 represents the permeability of vacuum and I denotes the current. Furthermore, $d\mathbf{l}^s$ represents an infinitesimal length element of the source, r is the distance from that source element, and $\mathbf{r}$ is the distance vector. The current I can be direct or alternating. However, the validity of the magnetic field presented in Equation (1) is limited to low frequencies and currents with sufficiently small changes(error analysis regarding the neglect of retardation and the assumption of the Biot-Savart law is provided in the Appendix A.). The force exerted by wire A on wire B can be determined using the Lorentz force law

$$\mathbf{F}_A^B = I_B \oint_B d\mathbf{l}^B \times \mathbf{B}_A \tag{2}$$

The convention used here, F_A^B, represents the force exerted by object A on object B. By converting the triple cross products to dot products, it follows

$$\mathbf{F}_A^B = \frac{\mu_0 I_A I_B}{4\pi} \left[\oint \oint \frac{d\mathbf{l}^A \left(d\mathbf{l}^B \cdot \hat{\mathbf{r}}_{BA} \right)}{r^2} - \oint \oint \frac{\hat{\mathbf{r}}_{BA} \left(d\mathbf{l}^B \cdot d\mathbf{l}^A \right)}{r^2} \right] \tag{3}$$

where $\hat{\mathbf{r}}_{BA} = (\mathbf{r}_B - \mathbf{r}_A)/r$ represents the unit vector pointing from the infinitesimal element $d\mathbf{l}^A$ toward $d\mathbf{l}^B$, and $r = |\mathbf{r}_B - \mathbf{r}_A|$ is the distance between these elements. The second term on the right-hand side of Equation (3) shows symmetry, and its contribution implies equal and opposite interaction on wires A and B.

We can write $d\mathbf{r} = d\mathbf{r}_B - d\mathbf{r}_A$. If we integrate first over B and then A, in the inner integral, we only move along wire B while the point on A is fixed. Hence we can write $d\mathbf{l}^B = d\mathbf{r}$. In the inner integral, by expanding the differentials in spherical coordinates it follows

$$d\mathbf{l}^B \cdot \hat{\mathbf{r}} = d\mathbf{r} \cdot \hat{\mathbf{r}} = dr \tag{4}$$

Using the identity (4), the force term (3) can be written as

$$\mathbf{F}_A^B = \frac{\mu_0 I_A I_B}{4\pi} \left[\oint_A d\mathbf{l}^A \oint_B \frac{dr}{r^2} - \oint \oint \frac{\hat{\mathbf{r}}_{BA} \left(d\mathbf{l}^B \cdot d\mathbf{l}^A \right)}{r^2} \right] \tag{5}$$

[7] The Biot-Savart law is a good approximation of the magnetic field if $\frac{1}{r^2 c} \frac{\partial I}{\partial t} \ll I/r^3$.

The closed integral $\oint \frac{dr}{r^2}$ equals zero for a closed wire. This is because the integration is performed over a closed loop on a differential. Conclusively, two closed loops exert equal and opposite forces on each other. The second integral in Equation (5) can be named the "reciprocal force," possessing symmetry and is directionally dependent on both wires interacting points. In contrast, the first term in Equation (5) can be termed the "directional force," as its direction depends only on one of the wires and exhibits asymmetry. As previously stated, the directional force vanishes for a closed loop.

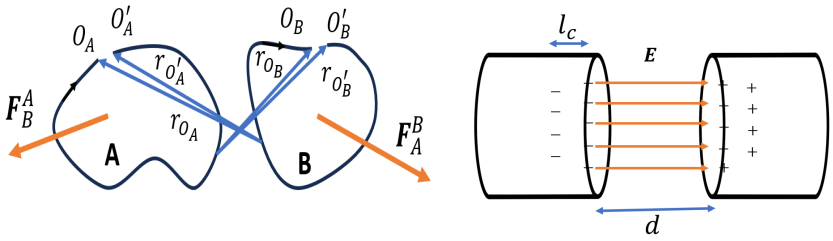

(a) (b)

Figure 1: (a) Diagram depicting two open-circuit wires, A and B, each with a disconnection point forming capacitive gaps (labeled as O_A and O'_A for wire A and O_B and $O'_B$for wire B). The $r_{O'_B}$ and r_{O_B} are the distance of any point on wire A from the open section on wire B. The interaction forces $\mathbf{F}_A^B$ and $\mathbf{F}_B^A$ may not be equal and opposite(reciprocal). (b) The capacitor formation by a distance gap of d in a segmented wire, with charge accumulating on both sides of the wire.

Now, consider two open-circuit wires (see Figure 1). Each wire has a specific disconnection point, with a sufficiently small gap that acts as a capacitor. This configuration allows current to flow based on the applied voltage and the charge accumulated at these disconnection points. Importantly, no discharge occurs between these disconnected points. The length of the zone where charges accumulate is close to the outer surface at disconnection points and is negligible compared to the gap length. Let's denote the disconnection points for wire A as O_A and O'_A, and for wire B as O_B and O'_B (moving in the direction of the current). The magnetic interaction forces on wires A and B by neglecting the capacitor zone(where charges accumulate) can be expressed as follows:

$$ {}^{M}\mathbf{F}_A^B = \frac{\mu_0 I_A I_B}{4\pi} \left[\int_A \left(\frac{1}{r_{O'_B}} - \frac{1}{r_{O_B}} \right) d\mathbf{l}^A - \int\int \frac{\hat{\mathbf{r}}_{BA} \left(d\mathbf{l}^B \cdot d\mathbf{l}^A \right)}{r^2} \right] \tag{6} $$

and

$$ {}^{M}\mathbf{F}_B^A = \frac{\mu_0 I_A I_B}{4\pi} \left[\int_B \left(\frac{1}{r_{O'_A}} - \frac{1}{r_{O_A}} \right) d\mathbf{l}^B - \int\int \frac{\hat{\mathbf{r}}_{AB} \left(d\mathbf{l}^B \cdot d\mathbf{l}^A \right)}{r^2} \right] \tag{7} $$

The superscript M shows the magnetic contribution of forces. Here, r_O denotes the distance between point O and the infinitesimal element on the other wire(see Figure 1). The reciprocal forces cancel each other. By neglecting the force on the capacitor zone, the magnetic net force between the two wires resulting from directional forces is then expressed as

$$ {}^{M}\mathbf{F}_{A}^{B} + {}^{M}\mathbf{F}_{B}^{A} = \frac{\mu_0 I_A I_B}{4\pi} \left[\int_A \left(\frac{1}{r_{O'_B}} - \frac{1}{r_{O_B}} \right) d\mathbf{l}^A + \int_B \left(\frac{1}{r_{O'_A}} - \frac{1}{r_{O_A}} \right) d\mathbf{l}^B \right] \tag{8} $$

It can be demonstrated that in many configurations, the net magnetic force between the open wires is nonzero. A clear illustration of this occurs when wire A and wire B lie in perpendicular planes, and the differential elements $d\mathbf{l}^A$ and $d\mathbf{l}^B$ are independent of each other.

Another aspect to consider is the magnetic field interactions resulting from the rearrangement and movement of charges in capacitors. This movement generates a magnetic field, and the magnetic field of other wires exerts force on the capacitors. Equation (8) does not account for this effect. If the capacitance is due to a small gap between two wires with strong dielectric material in between, the electric charge predominantly accumulates close to the outer surface, as shown in Figure 1(b). In such cases, the length of the capacitor zone, denoted as l_c, can be very small. During the charging or discharging processes, the charges rearrange both radially and along the axis of l_c. For thin wires and a small l_c relative to the gap distance d, the contribution of the magnetic force due to this rearrangement might be negligible, and Equation (8) can be applicable. However, in general, the magnetic force resulting from charge rearrangement in a capacitor should not be overlooked.

We will now provide general proof that the resultant magnetic force between a closed thin wire and a thin wire connected to an arbitrarily shaped capacitor is non-zero. Let's call the circuit with a closed wire "Circuit A" and the circuit with an open wire plus a capacitor "Circuit B." The domain of Circuit B can be decomposed into the wire section, denoted as B^{Wr}, and the capacitor section, denoted as B^{Cp} (please see Figure 2). As proven earlier, the directional force on the closed wire can be shown to be zero. It is sufficient to show that the directional force on the open wire and capacitor, regardless of the capacitor's shape, can be non-zero. Using the expression obtained for wires in Equation (8), considering that the reciprocal parts cancel each other out, and applying the Lorentz force to calculate the effect of Circuit A's magnetic field on the current density $\mathbf{J}$ in the capacitor's electrodes, we can write

$$ \begin{aligned} {}^{M}\mathbf{F}_{A}^{B} + {}^{M}\mathbf{F}_{B}^{A} &= \frac{\mu_0 I_A I_B}{4\pi} \oint_A \left(\frac{1}{r_{O'_B}} - \frac{1}{r_{O_B}} \right) d\mathbf{l}^A \\ &+ \frac{\mu_0 I_A}{4\pi} \oint_A \int_{B^{Cp}} \frac{d\mathbf{l}^A \left(\mathbf{J}^B \cdot \hat{\mathbf{r}}_{BA} \right)}{r^2} dv \end{aligned} \tag{9} $$

By writing $\frac{\hat{\mathbf{r}}_{BA}}{r^2} = -\nabla \frac{1}{r}$ and using the identity for the divergence of a scalar-

vector product, we obtain

$$\frac{\left(\mathbf{J}^B \cdot \hat{\mathbf{r}}_{BA}\right)}{r^2} = -\mathbf{J}^B \cdot \nabla \frac{1}{r} = -\operatorname{div}\left(\frac{\mathbf{J}^B}{r}\right) + \frac{\operatorname{div}\left(\mathbf{J}^B\right)}{r} \tag{10}$$

By applying the divergence theorem, we have

$$\int_{B^{Cp}} \operatorname{div}\left(\frac{\mathbf{J}^B}{r}\right) dv = \oint_{B^{Cp}} \frac{\mathbf{J}^B \cdot \mathbf{n}}{r} ds \tag{11}$$

where $\mathbf{n}$ is the normal to the surface of the domain containing the capacitor. If we assume the current density entering the capacitor through a very thin wire at point O_B can be expressed as $\mathbf{J}_B = -I_B \delta(\mathbf{r} - \mathbf{r}_{O_B})\mathbf{n}$ and the outward current density at point O'_B is $\mathbf{J}_B = I_B \delta(\mathbf{r} - \mathbf{r}_{O'_B})\mathbf{n}$, where δ is the Kronecker delta function, for thin wires, we can write

$$\oint_{B^{Cp}} \frac{\mathbf{J}^B \cdot \mathbf{n}}{r} ds = I_B \left(\frac{1}{r_{O_B}} - \frac{1}{r_{O'_B}}\right) \tag{12}$$

Using (9), (10), (11), and (12), we have

$${}^M\mathbf{F}_A^B + {}^M\mathbf{F}_B^A = \frac{\mu_0 I_A}{4\pi} \oint_A \int_{B^{Cp}} \frac{\operatorname{div}\left(\mathbf{J}^B\right)}{r} dv \, d\mathbf{l}^A \tag{13}$$

The continuity equation gives the identity $\operatorname{div}\left(\mathbf{J}^B\right) = -\frac{\partial \rho}{\partial t}$. Hence, the net force is a function of the rate of charge accumulation in the capacitor, and we finally obtain

$${}^M\mathbf{F}_A^B + {}^M\mathbf{F}_B^A = -\frac{\mu_0 I_A}{4\pi} \oint_A \int_{B^{Cp}} \frac{1}{r} \frac{\partial \rho}{\partial t} dv \, d\mathbf{l}^A \tag{14}$$

For thin capacitors with similar electrodes and when charges are uniformly distributed on both sides of the electrodes, the following relation can be given

$${}^M\mathbf{F}_A^B + {}^M\mathbf{F}_B^A = -\frac{\mu_0 I_A I_B}{4\pi S} \oint_A \int_{B_s^{Cp}} \left(\frac{1}{r^+} - \frac{1}{r^-}\right) ds \, d\mathbf{l}^A \tag{15}$$

Where S is the area of the surface of the capacitor's electrode and r^+ and r^- is the distance of wire A from positive and negative charges respectively. When we have a closed wire and an open wire with a small gap, Equation (8) can be recovered from Equation (15) by assuming charge accumulation is close to the surface of discontinuity.

A valid question to consider is: if we treat the open sections as a capacitor, what effect does the electric field have on the net force? It is trivial to assume that the force on the accumulated charge at both ends of the open sections cancels out [8]. There is a corresponding charge at the other end for every charge on one side of the capacitor.

[8] There is a possible asymmetrical interaction due to electrostatic pressure (Biefeld-Brown Effect), as widely discussed in [22, 23]. However, this effect is extremely small and can be neglected if symmetrical capacitors are selected. Secondly, as will be further discussed, the magnetic forces generated can be in a different direction than the induced electric pressure forces and are independent.

Aside from electric fields resulting from charges, changes in current can also cause electric fields. The induced electric field resulting from circuit A using Jefimenko's equations and neglecting retardation can be described by the equation

$$\mathbf{E}_{ind} = -\frac{\mu_0}{4\pi}\int \frac{1}{r}\left[\frac{\partial I}{\partial t}\right] d\mathbf{l}^s. \tag{16}$$

While induced electric field resulted from circuit A exert force on charges, the charges on capacitors does not produce any force on the wire. Hence, for the electric fields, it can be written

$${}^{E}\mathbf{F}_A^B + {}^{E}\mathbf{F}_B^A = -\frac{\mu_0}{4\pi}\oint_A \int_{B^{Cp}} \frac{\rho}{r}\frac{\partial I_A}{\partial t} dv\, d\mathbf{l}^A \tag{17}$$

We can neglect the induced electric field when the rate of current I_A is small.

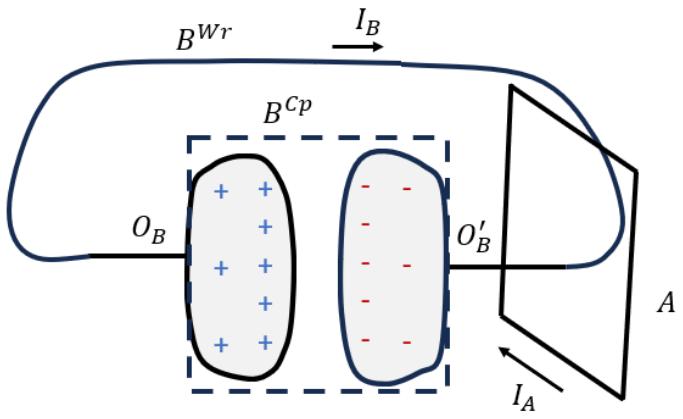

(a)

Figure 2: Schematics of Circuit A, a closed-loop wire carrying current I_A, and Circuit B, an open-loop wire defined by B^{Wr} and carrying current I_B, along with a capacitor of arbitrary shape in region B^{Cp}.

Earlier, we used Biot-Savart law to describe magnetic fields of wires, which neglects the radiative terms. Without introducing complexity to our equation, we can now write the general form of the magnetic field around the wire by including radiation terms (still retardation is neglected)

$$\mathbf{B} = \frac{\mu_0}{4\pi}\oint \left(\frac{[I]}{r^3} + \frac{1}{r^2 c}\left[\frac{\partial I}{\partial t}\right]\right) d\mathbf{l}_s \times \mathbf{r} \tag{18}$$

The magnetic force resulting from the magnetic radiation field (second term on right-hand side of Equation (18)) can be shown to be

$${}^{M}_{\text{rad}}\mathbf{F}_A^B + {}^{M}_{\text{rad}}\mathbf{F}_B^A = \frac{\mu_0}{4\pi c}\oint_A \int_{B^{Cp}} ln\,(r)\,\frac{\partial I_A}{\partial t}\frac{\partial \rho}{\partial t} dv\, d\mathbf{l}^A \tag{19}$$

Where c is the speed of light, the radiative(far field) magnetic force usually decays much slower because of the term $ln(r)$. This shows that a closed wire with an alternating current can have a far-field effect on the antenna's transmitter or circuits with capacitors. However, this effect is extremely small because of the term c in the dominator.

Combining all magnetic fields forces (19) and (14) and electric forces (17) results in this expression

$$\mathbf{F}_A^B + \mathbf{F}_B^A = -\frac{\mu_0}{4\pi} \oint_A \int_{B^{Cp}} \frac{1}{r} \frac{\partial (\rho I_A)}{\partial t} dv \, d\mathbf{l}^A + \frac{\mu_0}{4\pi c} \oint_A \int_{B^{Cp}} ln\,(r) \frac{\partial I_A}{\partial t} \frac{\partial \rho}{\partial t} dv \, d\mathbf{l}^A \tag{20}$$

An unjust and inaccurate statement about these types of electromagnetic setups is that the force only can result from an asymmetric radiation pattern and that radiative momentum causes the induced force, similar to what occurs in antennas. When momentum gain relies solely on radiation(in far distances), the momentum P to energy E expenditure in such cases is extremely small or $|P|/E = 1/c$. However, we observe that when $\frac{\partial I_A}{\partial t}$ is zero or very small and radiative terms vanish or are small, a net force can still result from non-radiative (near field) terms, which can contribute to momentum gain more efficiently. In this case, the energy loss is mainly due to loss to the resistance of the conductor than field radiation. Non-radiative fields do not propagate energy from their source, and the energy spent on producing fields is recoverable.

2.2 Non-zero Effects of Self-induced Stress Tensors and Linear Momentum Change

Previously, it was shown that the forces between two open wires with capacitors are non-reciprocal and may not cancel each other out. Now, let's examine this phenomenon from another perspective.

There is a common idea in physics that, in the absence of external forces, the total linear momentum of any isolated system remains constant. As stated in [24], "A closed system is one that can be enclosed in a surface upon which all components of the stress-energy tensor can be neglected." In simpler terms, for a closed system, there should be no effective momentum flux density (stresses) and energy flux from the boundaries into the system. The stress tensor can be any type of external stress, including mechanical stresses, which are essentially electromagnetic stresses at the atomic level.

This definition of a closed system leads to a general principle in special relativity known as the center of energy theorem. This theorem states that if the center of energy of a closed system is at rest, then its total momentum is zero [24, 25, 26]. When there is no external contribution of stress from external masses and bodies, we expect the stress contributions to be zero on the surface of the closed system.

However, what is often overlooked in the derivation of these principles is the possibility of asymmetries arising from the self-induced stresses of the system, which can act on the boundaries. Commonly, it is expected that the sum of self-

induced stresses on the surface of an enclosed system is zero. A typical example is a charged sphere with a uniform charge distribution and uniform electrostatic pressure. Despite the existence of electrostatic pressure, the symmetrical self-induced stresses lead to no net-induced force.

For an arbitrary closed surface containing two stationary point charges, the stress tensors (in this case, electrostatic pressure) may not be distributed homogeneously on the surface. Nevertheless, it can be shown that the sum of all stresses on an arbitrary enclosed surface is zero, and we can expect the center of mass of these charges not to move. However, can there be a scenario where the sum of self-induced stress tensors on its surface is non-zero?

Examining Maxwell stress tensors to assess the momentum equilibrium state of electromagnetic systems is a fundamental approach and is a common practice in engineering applications [27, 28]. We aim to demonstrate that the sum of self-induced stress tensors for any closed surface enclosing discontinuous wires with current is non-zero, and consequently, the total linear momentum can change (for a full description of the wires set-up, see Figure 2).

The Maxwell magnetic stress tensor can be defined through

$$\boldsymbol{\sigma}^B = \frac{1}{\mu}\mathbf{B}\otimes\mathbf{B} - \frac{1}{2\mu}B^2\mathbf{I} \tag{21}$$

Where $\mathbf{I}$ is the second-order identity tensor. Similarly, we can define the electric stress tensor as

$$\boldsymbol{\sigma}^E = \epsilon_0\mathbf{E}\otimes\mathbf{E} - \frac{\epsilon_0}{2}E^2\mathbf{I} \tag{22}$$

Where ϵ_0 is the vacuum permittivity. The equation for the conservation of momentum in the Eulerian perspective, including both electromagnetic and mechanical momentum, according to [1][9], can be written as

$$\oint_S \boldsymbol{\sigma}.d\mathbf{a} = \frac{d\left(\mathbf{P}_m + \mathbf{P}_{em}\right)}{dt} = \frac{d\mathbf{P}_{tot}}{dt} \tag{23}$$

where $\mathbf{P}_m$ is mechanical and $\mathbf{P}_{em}$ is electromagnetic momentum defined through

$$\mathbf{P}_{em} = \frac{1}{\mu_0 c^2}\int_v \mathbf{E}\times\mathbf{B} \tag{24}$$

Here, c is the speed of light in a vacuum. Assume the integral is done over any arbitrary surface S enclosing the two circuits A (closed) and B with capacitor (see Figure 2). It is assumed the fringing effect of electric fields at the discontinuity is negligible, and the electric field from charge accumulations is only present between the gaps and is zero on the surface S. It is also assumed the stress tensors resulting from induced electric fields are negligible since the rate of current change in a closed loop is small. Thus, it is assumed that magnetostatic stresses predominantly influence the surface S[10]. The low rate of current change

[9] See 8.28 and 8.30 in [1].

[10] This assumption is invalid if we move far from the wires where the magnetostatic terms decay faster than radiative terms. At far distances, stresses approach zero, and the surface area approaches infinity, resulting in an indeterminate form. We cannot simply assume, at infinity, stress tensors vanish.

also allows us to neglect the radiative terms of magnetic field in stress tensor. We will further observe, by neglecting radiative terms, the effect of self-induced stress tensor is not dependent on the chosen surfce S.
Using the divergence theorem for second-order tensors, we have

$$\oint_S \boldsymbol{\sigma}.d\mathbf{a} = \int_v \nabla.\boldsymbol{\sigma} dv \tag{25}$$

where the magnetic field resulted from two wires on any point with position $\mathbf{r}$ using superposition can be written as

$$\mathbf{B} = \frac{\mu_0}{4\pi} \int_v \left[\frac{\mathbf{J}^s \times \left(\mathbf{r} - \mathbf{r}_s^A\right)}{|\mathbf{r} - \mathbf{r}_s^A|^3} + \frac{\mathbf{J}^s \times \left(\mathbf{r} - \mathbf{r}_s^B\right)}{|\mathbf{r} - \mathbf{r}_s^B|^3} \right] dv \tag{26}$$

By neglecting the retardation effects, Equation (26) can be rewritten in the form

$$\mathbf{B} = \frac{\mu_0}{4\pi} \nabla \times \int_v \left[\frac{\mathbf{J}^s}{|\mathbf{r} - \mathbf{r}_s^A|} + \frac{\mathbf{J}^s}{|\mathbf{r} - \mathbf{r}_s^B|} dv \right] \tag{27}$$

and from Equations (25) and (26) and using the gradient of dot product identity, it can be written

$$\nabla.\boldsymbol{\sigma}^B = \frac{1}{\mu_0} \left[(\mathbf{B}.\nabla)\mathbf{B} - \frac{1}{2}\nabla B^2 \right] = -\frac{1}{\mu_0} \left[\mathbf{B} \times (\nabla \times \mathbf{B}) \right] \tag{28}$$

using curl of curl identity which is $\nabla \times (\nabla \times \mathbf{A}) = \nabla (\nabla \cdot \mathbf{A}) - \nabla^2 \mathbf{A}$ and considering that we have $\nabla^2 1/|\mathbf{r} - \mathbf{r}_s| = -4\pi\delta(\mathbf{r} - \mathbf{r}_s)$, we can write

$$\begin{aligned} \nabla \times \mathbf{B} &= \mu_0 \int_v \left[\delta(\mathbf{r} - \mathbf{r}_s^B)\mathbf{J}^s + \delta(\mathbf{r} - \mathbf{r}_s^B)\mathbf{J}^s \right] dv \\ &- \frac{\mu_0}{4\pi} \int_v \left[\mathbf{J}^s \cdot \nabla \frac{\left(\mathbf{r} - \mathbf{r}_s^A\right)}{|\mathbf{r} - \mathbf{r}_s^A|^3} + \mathbf{J}^s \cdot \nabla \frac{\left(\mathbf{r} - \mathbf{r}_s^B\right)}{|\mathbf{r} - \mathbf{r}_s^B|^3} \right] dv \end{aligned} \tag{29}$$

The second term in the bracket in the integral (29) vanishes. For each component of the term in the bracket [11], it can be written (for instance, in the x direction)

$$\int \mathbf{J}^s \cdot \nabla \frac{(x - x_s)}{|\mathbf{r} - \mathbf{r}_s|^3} dv = \int \nabla \cdot \left(\frac{(x - x_s)}{|\mathbf{r} - \mathbf{r}_s|^3} \mathbf{J}^s \right) dv = -\int \nabla_s \cdot \left(\frac{(x - x_s)}{|\mathbf{r} - \mathbf{r}_s|^3} \mathbf{J}^s \right) dv = 0 \tag{30}$$

By using the divergent theorem and considering that no current is entering the boundary of the integral domain, the last term in Equation (30) equates to zero.

By using the divergence theorem and considering that no current is entering the boundary of the integral domain, the last term in Equation (30) equates to zero. Using Equations (28), (29) and (30) we an write:

$$\int \nabla.\boldsymbol{\sigma} dv = -\frac{1}{\mu_0} \int \mathbf{B} \times (\nabla \times \mathbf{B})\, dv = \int \left(\mathbf{J}^s \left(\mathbf{r}_s^A\right) + \mathbf{J}^s \left(\mathbf{r}_s^B\right) \right) \times \mathbf{B}\, dv \tag{31}$$

[11] $\mathbf{J}_s$ is function of the position of source $\mathbf{r}_s$ and the derivatives of $\mathbf{J}_s$ vanishes with respect to ∇ which is independent of coordinates of the source(x_s, y_s, z_s) and consequently here we can write $\mathbf{J}_s \cdot \nabla\psi = \nabla \cdot (\psi \mathbf{J}_s)$ if ψ is a scalar.

Where $\mathbf{J}^s(\mathbf{r}_s)$ indicates that the charge density is only nonzero at its source. Here, we can assume $\mathbf{J}^s dv = Id\mathbf{l}^s$ for wires and the same magnetic field cannot interact with its own source(cause) [12], The right-hand side of Equation (31) basically give the Lorentz magnetic interaction force which earlier we proved that is non-zero, and finally we have

$$\oint_S \boldsymbol{\sigma}.d\mathbf{a} = \int \nabla.\boldsymbol{\sigma} dv = {}^M\mathbf{F}_A^B + {}^M\mathbf{F}_B^A \tag{32}$$

Finally from Equations (23) and (32) we can write:

$${}^M\mathbf{F}_A^B + {}^M\mathbf{F}_B^A = \frac{d\mathbf{P}_{tot}}{dt} \tag{33}$$

Equation (32) clearly illustrates that the effect of self-induced stress tensors may not generally be zero on an arbitrary surface around an electrical object and can lead to a change in total momentum. On the contrary, when there is no discontinuity, we expect no change in total momentum, and we may expect the center of mass/energy to exhibit steady motion. In [29], it is suggested that in order to justify the "missing symmetry" in Newton's third law, a force from the vacuum should be considered. Here, we observe that this force is not from the vacuum but from the interaction and asymmetries of the fields themselves on the boundaries. Given that the resultant stress tensors of a system on its own boundary are not always zero, we may need to assume that matter and fields do not form a closed system in our case and many other possible scenarios.

In our application, $\mathbf{P}_{em}$ has a very subtle contribution to a change of momentum, and its effect is in order of $\sim 1/c^2$ as Equation (24) suggests. Hence, it can be written

$$\mathbf{F}_A^B + \mathbf{F}_B^A \approx \frac{d\mathbf{P}_m}{dt} \tag{34}$$

2.3 Example of circular capacitor and non-reciprocal magnetic force interaction

For simplicity, in the case of large capacitors, this work examines the force exerted by a closed wire on a circular capacitor and vice versa. We will demonstrate the breaking of the reciprocity of forces, which can lead to a resultant force. This force can be derived from the distribution of input and output current densities on the capacitor's boundary and the charge density distribution within the capacitor, as outlined in Section 2.1, or directly from the current density distribution within the capacitor. Both approaches are equivalent. We assume that the charge is symmetrically distributed on the circular plate. The capacitor is sufficiently charged such that the electrostatic forces predominantly determine the charge distribution, while the influence of nearby current-carrying wires on this distribution is considered negligible. Consider that the outer radius of the capacitor is R, and the inner radius a is equal to that of the thin

[12] Fields propagate from its cause and displace, making it impossible to interact with its own cause at the same time

wire(a can approach zero for an ideal thin wire). By neglecting fringing effects, the density of the charge per unit thickness of the capacitor can be described as follows

$$\rho = Q(t)/(\pi(R^2 - a^2)) \tag{35}$$

The Q is the charge on the plate, and the rate of change of charge on the plate is equal to the current entering the capacitor. The balance of charge in the circular plate necessitates

$$\frac{\partial \rho}{\partial t} + \nabla \cdot \boldsymbol{J} = 0 \quad \text{and } \boldsymbol{J}(R) = 0 \tag{36}$$

Due to radial symmetry, the divergence operator $\nabla \cdot \boldsymbol{J}$ simplifies in polar coordinates to $\frac{1}{r'}\frac{\partial\,(r' J_{r'})}{\partial r'}$. Where r' is the distance from the center of the capacitor's electrode. With reference to the charge density equation (Equation (35)) and the continuity equation (Equation (36)), we can derive the following relationship [13]:

$$J_{r'} = \frac{1}{2}\frac{I_B}{\pi(R^2 - a^2)}\left(\frac{R^2}{r'} - r'\right) \tag{37}$$

Where I_B is the current entering and exiting the capacitor, as shown in Figure 3, the current density distribution allows us to define the magnetic field around the capacitor. There is a misconception that displacement current is primarily responsible for the magnetic field around a capacitor. However, as correctly mentioned in [30], the conduction current is the primary source of the magnetic field within a capacitor. Maxwell's displacement current does not cause the magnetic field but complements the relationship between current and magnetic field in Ampère's Law. In other words, Maxwell's displacement current is essential for the propagation of electromagnetic waves and the continuity of the fields, but it is not the causal factor. Consequently, the magnetic field of the capacitor electrode is obtained from its distributed current density. The proof that the magnetic field, derived from the charge and current density equations using the Biot-Savart law, satisfies the Ampère-Maxwell law is provided in Appendix B.

In our application, the capacitor has two key roles. First, it ensures the continuity of the electric field throughout the entire circuit. Second, it breaks the symmetry of the force interaction.

To calculate the magnetic field caused by the current density inside the circular capacitor, we can employ the Biot-Savart Law as follows [14]

$$\mathbf{B}_C = \frac{\mu_0}{4\pi}\int_0^{2\pi}\int_a^R \frac{(\hat{\mathbf{r}}' \times \hat{\mathbf{r}})}{r^3} r' J_{r'} dr' d\theta \tag{38}$$

Here, $\mathbf{r} = \mathbf{r}_{MA} + \mathbf{r}'$ and $\mathbf{r}_{MA}$ represents the distance from the center of the capacitor to wire A, and the hat symbol denotes the unit vector. The vector $\mathbf{r}'$

[13] The fact that the current density in equation (37) is approximated here does not invalidate the forthcoming general proof demonstrating the non-reciprocal interaction between the wire and the capacitor.

[14] In case we do not have symmetry, we can add the current density $J_{\theta'}$ in angular direction $\hat{\theta}'$.

indicates the distance from the center of the capacitor to a corresponding point on the capacitor (as shown in Figure 3). The force exerted by closed wire A (as shown in Figure 3) on one side of capacitor C can be derived from the Lorentz force equation as follows

$$\begin{aligned} {}^{M}\mathbf{F}_{A}^{C} &= \frac{\mu_0 I_A}{4\pi} \oint_A d\mathbf{l}^A \int_0^{2\pi} \int_a^R \frac{\left(\hat{\mathbf{r}'} \cdot \hat{\mathbf{r}}\right)}{r^2} r' J_{r'} dr' d\theta \\ &- \frac{\mu_0 I_A}{4\pi} \oint_A \int_0^{2\pi} \int_a^R \frac{\hat{\mathbf{r}} \left(\hat{\mathbf{r}}' \cdot d\mathbf{l}^A\right)}{r^2} r' J_{r'} dr' d\theta \end{aligned} \tag{39}$$

The first integral in Equation (39) depends on the direction of the current in wire A. Meanwhile, the second term demonstrates reciprocity; its direction is independent of the currents' direction and aligns with the line connecting interaction points.

It can easily be shown that the directional force of the capacitor on a closed wire A is zero. Then, the sum of the force of wire A on the capacitor electrode and the capacitor electrode on wire A is nonzero (reciprocity breaks) and is given by [15]

$${}^{M}\mathbf{F}_{A}^{C} \; + \; {}^{M}\mathbf{F}_{C}^{A} = \frac{\mu_0 I_A}{4\pi} \oint_A d\mathbf{l}^A \int_0^{2\pi} \int_a^R \frac{(\hat{\mathbf{r}}' \cdot \hat{\mathbf{r}})}{r^2} r' J_{r'} dr' d\theta \tag{40}$$

The capacitor can be considered analogous to open wires, where charge flows radially from the center to the edges. Consequently, we can expect that the sum of the forces will not be reciprocal, as is the case with open wires.

When symmetries are considered, a wire with its own capacitor may not produce force on itself. For instance, the net force resulting from the interactions between wire B and its attached capacitor can be demonstrated to be zero when the capacitors at both ends of the disconnection point are identical and the wire setup is symmetrical concerning the capacitor's mid-plane.

In summary, we have shown that the force between an open and a closed wire and between a capacitor and a closed wire is non-reciprocal. The electric field interactions resulting from charge accumulations are assumed to be reciprocal, and the magnetic self-force is assumed to be zero when symmetries are considered.

[15] If the conducted current in the capacitor lacks symmetry, an angular direction term can be added to the inner integral for generality.

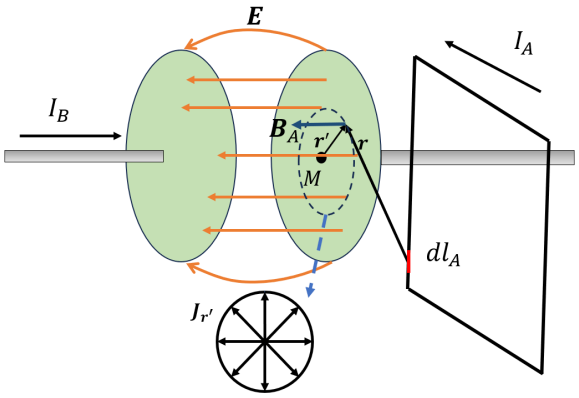

(a)

Figure 3: Depiction of the electric field between two plates of the capacitor and the radial current density distribution in a circular capacitor. The interaction between a differential element dl_A and a point on the capacitor is depicted through the magnetic field B_A and the current density $J_{r'}$.

3 Examples and Discussions

Consider a scenario where alternating current (AC) passes through a primary circuit with two open sections. A circular capacitor with a dielectric material is placed within these openings with no electrical discharge. The circuit voltage is sufficient to maintain the current flow in the primary circuit. Secondary circuits are positioned near the main circuit's open segments to produce a net force in the desired direction. These secondary circuits can operate in-phase or out-of-phase with the primary circuit depending on the intended force direction. System symmetries are designed to eliminate any potential net moment. Figure 4 provides a circuit schematic. O and O' denote the open section. Secondary circuits are placed near the open sections to the right and left of the primary circuit.

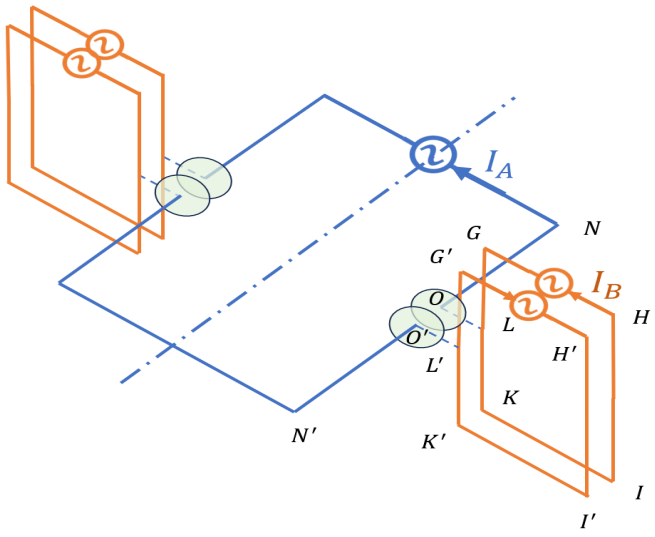

Figure 4: A simplified diagram of a novel AC-powered propulsion system. Capacitors are placed at open sections between points O and O' while secondary circuits are positioned for upward directional force generation. Secondary circuits are identical and symmetrical with respect to the main circuit plane (i.e., GL = LK).

The circuit design presented in Figure 4 aims to produce a net upward force. Segments GH and IK, as well as $G'H'$ and $I'K'$, negate each other's effects. KG and $K'G'$ contribute the most to the upward force, while HI and $H'I'$ have lesser contributions due to their distances, as outlined in equations (7) or (6). The alternative current in circuit $GHIK$ is out-of-phase with that of $G'H'I'K'$ to prevent force cancellation. A sinusoidal AC profile has been selected for this purpose. There are no limitations on the number of open sections or turns in either the primary or secondary circuits, allowing for scalable force generation. However, we'll consider a simple application here. An alternating current of $|I_A| = |I_B| = 1000$ amps is used for both the primary and secondary circuits. The distance between O and O' varies, and GL and LK lengths are chosen $15cm$ each. To minimize counteracting forces from opposing current, the wire HI is positioned further away, at a distance of 25 cm. The secondary circuits are positioned opposite on each side to cancel out the moment produced in the main circuit and maintain symmetry. The capacitor radius has been set at 0.8 cm. This small size was chosen primarily to focus on the forces exerted by the wires on each other. However, there is no limitation on the size of the capacitor. The

net force is computed numerically from the Equations (8) and (40) [16]. Figure 5(a) illustrates the average net force for varying distances between point L (in the secondary circuits) and the main circuit. Figure 5(b) illustrates the effect of distance between the gap OO' on produced average net force. Increasing the gap distance introduces more asymmetries, thereby increasing the resultant force. However, there are inherent limitations to increasing this distance due to specific system characteristics, such as the required voltage and the capacitance of the capacitors.

The alternating current in the circuit with the capacitor is assumed to have a sinusoidal profile, while a square-wave profile is used for the closed wire, alternating its sign at half the period of the sinusoidal wave. Consequently, the force generated in the system is proportional to $|\sin(\omega t)|$, where ω denotes the frequency of the alternating current. The average force for the sinusoidal profile is frequency-independent and reaches $\frac{2}{\pi}$ of the maximum force.

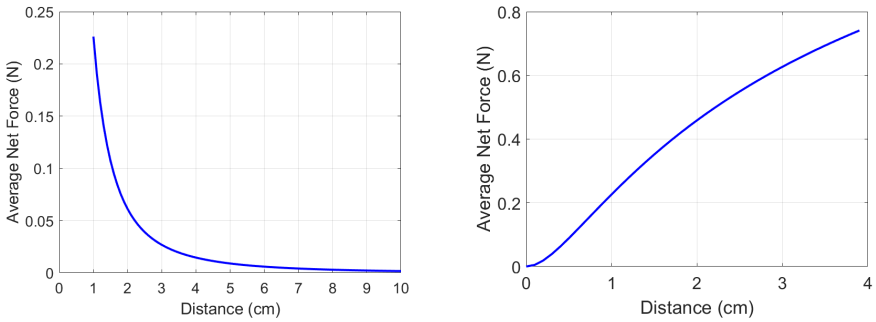

(a) (b)

Figure 5: The average net force produced in the setup depicted in Figure 4, as a function of (a) the distance between secondary and main circuits (with a fixed $OO' = 1cm$) (b) the OO' distance (with a fixed initial distance of 1 cm between the main and secondary circuits). Larger distances induce more asymmetries, leading to larger forces. However, there is always a limit to increasing the distance between the electrodes of capacitors due to the need for high voltages.

To understand how open sections can break force symmetry, consider the contribution of directional force (described by the first integral in Equation (3)) exerted by a unit length at the midpoint of line KG on a unit length along

[16] In practice, mutual coupling inherently exists between wire systems, potentially affecting the uniformity of current distribution. However, our calculation assumes weak coupling due to specific factors: secondary wire currents are perpendicular to the primary current, minimizing their impact on the produced electromotive force (EMF). Additionally, the two secondary wires are out of phase, canceling each other's influence. Based on these assumptions, the current distribution is imposed uniformly within the circuit rather than derived from solving a coupled system. While this simplifies the model, it does not undermine the fact that net force generation is possible, as outlined in the previous section.

line NN'. This force is plotted for continuous and discontinuous (with open sections) cases. Figure 6(a) illustrates the symmetry of directional forces in a continuous wire, leading to overall cancellation and no net force production. In contrast, Figure 6(b) demonstrates how open sections break this symmetry, resulting in a nonzero net force. In practice, when there are no open sections, fixing secondary circuits and allowing the primary circuit to rotate creates an electric motor that produces net torque on the primary circuit. This force is produced by coupled forces that cancel each other out. By omitting the part of the wire that carries force and by introducing a gap, the force symmetries break, consequently resulting in a non-zero directional force (small thrust) and rotation. The induced moments on the primary circuit can be canceled by introducing appropriate symmetries in the circuit setup, ultimately yielding a net thrust.

To effectively mitigate the capacitive reactance in the circuit, it is possible to use a two-element LC circuit by adding an appropriate inductor and setting the main circuit's operating frequency to match its natural resonant frequency. The design of the secondary circuit can also be modified to match this frequency. The power of proposed propulsion systems can be significantly enhanced by incorporating multiple turns and open sections. For example, using 20 turns and 20 sets of open sections instead of one can increase the forces depicted in Figure 5 by a factor of 400. For instance, by selecting a distance of 1 cm for the open section gap and the distance between the secondary and the primary circuits, we could potentially generate a force of approximately 80 Newtons. This force is sufficient to accelerate a probe with the mass of Voyager 1 (approximately 722 Kg) [31] such that it reaches the same distance traveled by Voyager 1 (up to January 2024) in less than a year [17]. This cannot be achieved with traditional propellant-based propulsion systems, as they require a vast amount of mass for constant acceleration.

Incorporating superconductors into this propulsion system could provide significant advantages and expand its potential applications to include terrestrial and aviation transportation. Unlike traditional electric motors, which lose energy through friction within their mechanical parts, this proposal eliminates such losses due to its lack of moving components. This characteristic paves the way for a highly efficient propulsion systems.

[17] This hypothetical example assumes that the equipment providing energy is not attached to the probe. The emphasis is on demonstrating how a small but constant force, over time, can generate sufficient velocity to traverse vast distances. However, the primary challenge isn't the amount of thrust but the energy required to achieve very high kinetic energy. A probe can have thousands of open sections and wire turns instead of the twenties mentioned in the example. The force is scalable, but ultimately, the needed energy is the limiting factor. Another proposal involves allowing the probe to orbit the sun, converting solar energy into kinetic energy by accelerating and increasing speed as it moves to orbits with higher escape velocities.

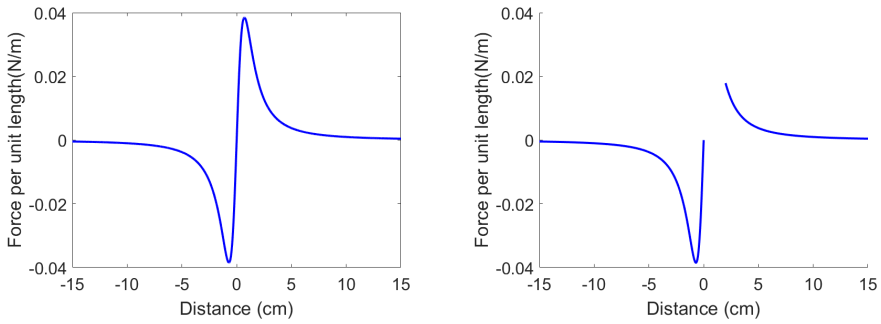

Figure 6: Directional force exerted by a unit length at the midpoint of line KG on a unit length along line NN' for two cases: (a) no open sections, and (b) a $2cm$ gap for the open section. The gap causes symmetry breaking. The maximum current in both main and secondary circuits is 1000 amps.

4 Conclusions

This research explored the breaking of symmetry in interaction forces of discontinuous circuits. It is demonstrated that in closed circuits, force interactions adhere to classical physics' expectations of reciprocity. Contrarily, this symmetry breaks in discontinuous circuits and can lead to a resultant magnetic force. Additionally, asymmetries in self-induced stress tensors are shown to change the total linear momentum. These asymmetries in self-induced stress tensors can generate a non-zero effect on the boundary of the surface enclosing wires, akin to external stresses produced by external fields. This phenomenon is often overlooked in the momentum equations of isolated bodies. A numerical example is provided, demonstrating that the resultant force can reach significant levels, making such systems suitable for aerospace applications.

MATLAB Code Availability

The MATLAB code used for plotting Figure 5(a) can be accessed and downloaded from the following GitHub repository:

Magnetic Force Generation MATLAB Code

This repository contains the full implementation of the numerical procedures described in this paper. Other plots can be generated with a slight modification of this code.

Acknowledgments

This work was conducted without external financial support. I am grateful to Professor Houshang Ardavan (Institute of Astronomy, University of Cambridge), Professor Richard Syms (Department of Electrical Engineering, Imperial College London), and Professor Kirk T. McDonald (Princeton University) for their valuable discussions, comments, and feedback.

Appendix A.

The Biot-Savart law, as presented in Methods section 2, provides an approximation of the actual magnetic fields. This appendix aims to analyze the error introduced by this approximation. The exact solution of the magnetic field around an infinitesimal wire is given by [21]:

$$d\mathbf{B} = \frac{\mu_0}{4\pi}\left(\frac{[I]^{ret}}{r^3} + \frac{1}{r^2 c}\left[\frac{\partial I}{\partial t_s}\right]^{ret}\right) d\mathbf{l}_s \times \mathbf{r} \tag{A.1}$$

The retardation symbol, $[]^{ret}$, indicates the state of the source element located at coordinates (x_s, y_s, z_s) at the retarded time, as observed from the point (x, y, z). For instance, the current at coordinate-time (x, y, z, t) refers to the state of the source at coordinate-time $(x_s, y_s, z_s, t - r/c)$:

$$[I(x, y, z, t)]^{ret} = I(x_s, y_s, z_s, t - r/c) \tag{A.2}$$

Fortunately, the time-dependent terms affect only the magnitude of the measured magnetic field and not its direction. To investigate the error introduced by neglecting these terms, it is sufficient to measure the error in the magnitude of the magnetic field. In this analysis, the error is examined for alternating current with a frequency of ω. At time t_0, the terms $[I]^{ret}$ can be approximated by:

$$[I]^{ret} = I(t_0) - \left.\frac{\partial I}{\partial t}\right|_{t_0}(r/c) + \left.\frac{\partial^2 I}{\partial t^2}\right|_{t_0}(r/c)^2 + \cdots \tag{A.3}$$

and

$$\left[\frac{\partial I}{\partial t}\right]^{ret} = \left.\frac{\partial I}{\partial t}\right|_{t_0} - \left.\frac{\partial^2 I}{\partial t^2}\right|_{t_0}(r/c) + \left.\frac{\partial^3 I}{\partial t^3}\right|_{t_0}(r/c)^2 + \cdots \tag{A.4}$$

For an alternating current, the current can be expressed as $I = I_0 \sin(\omega t)$. The magnetic field, according to the Biot-Savart law, is denoted by $\mathbf{B}^{Biot}$. The relative error introduced by assuming the Biot-Savart law over $t \in [0, T]$, where $T = \frac{2\pi}{\omega}$, for different angular frequencies and distances, can be measured as:

$$Error = \frac{\int_0^T \left\| d\mathbf{B} - d\mathbf{B}^{Biot} \right\| dt}{\int_0^T \left\| d\mathbf{B} \right\| dt} \tag{A.5}$$

where the differential $d\mathbf{l}_s$ in nominator and denominator cancels out. The fact that the approximation only affects the magnitude of the magnetic field led us to derive the approximation formula given in Equation (A.5). The relative error introduced as a function of frequency is plotted in Figure A1 for different distances from the source. The plot indicates that for distances less than 1 meter and frequencies below 1 MHz, the error remains approximately less than 1×10^{-4}. This implies that for calculations made under these conditions, the error will be negligible and should not significantly influence the overall conclusions drawn in this work.

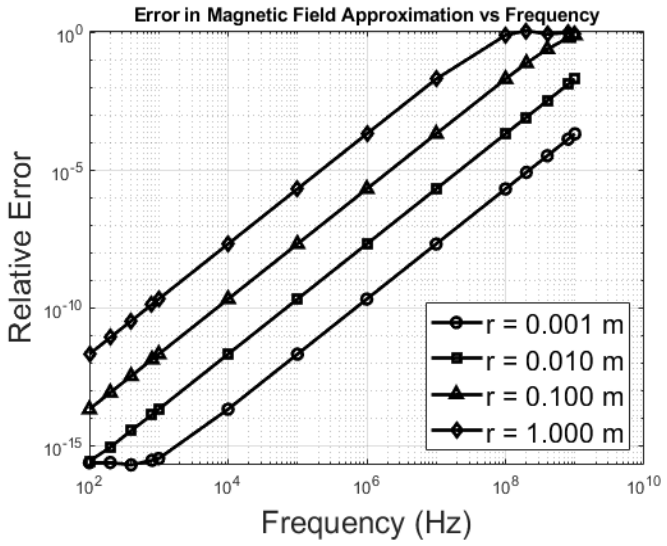

Figure A1: Relative error in magnetic field estimation due to the Biot-Savart law assumption for different frequencies and distances.

Appendix B.

This appendix presents the proof that the magnetic field derived from the charge and current density equation in the capacitor, along with the Biot-Savart law, satisfies the Ampère-Maxwell law. The electric field around the capacitor C at any point with position $\mathbf{r}$, neglecting negligible radiative terms and retardation effects, can be described by

$$\mathbf{E} = -\frac{1}{4\pi\epsilon_0}\nabla \int_V \frac{\rho_s}{|\mathbf{r} - \mathbf{r}_s^C|} dv_s \tag{B.1}$$

Here, $\mathbf{r}_s^C$ is the position vector corresponding to a point on capacitor C and ρ_s is the source charge density. Similarly, the magnetic field, neglecting radiative

terms and retardation effects, is given by

$$\mathbf{B} = \frac{\mu_0}{4\pi} \nabla \times \int_V \frac{\mathbf{J}^s}{|\mathbf{r} - \mathbf{r}_s^C|} dv_s \tag{B.2}$$

Now, considering the charge continuity equation

$$\nabla \cdot \mathbf{J}^s = -\frac{\partial \rho_s}{\partial t} \tag{B.3}$$

The displacement field $\mathbf{D}$ can be written as

$$\frac{\partial \mathbf{D}}{\partial t} = \epsilon_0 \frac{\partial \mathbf{E}}{\partial t} = \frac{1}{4\pi} \nabla \int_V \frac{\nabla_s \cdot \mathbf{J}^s}{|\mathbf{r} - \mathbf{r}_s^C|} dv_s \tag{B.4}$$

By applying the divergence theorem and noting that no current enters the boundary of the integral domain, we obtain

$$\begin{aligned} &\int_V \nabla_s \cdot \left(\frac{\mathbf{J}^s}{|\mathbf{r} - \mathbf{r}_s^C|} \right) dv_s = 0 \quad \Rightarrow \\ &\int_V \frac{\nabla_s \cdot \mathbf{J}^s}{|\mathbf{r} - \mathbf{r}_s^C|} dv_s = -\int_V \mathbf{J}^s \cdot \nabla_s \left(\frac{1}{|\mathbf{r} - \mathbf{r}_s^C|} \right) dv_s \end{aligned} \tag{B.5}$$

Given that:

$$\nabla_s \left(\frac{1}{|\mathbf{r} - \mathbf{r}_s^C|} \right) = -\nabla \left(\frac{1}{|\mathbf{r} - \mathbf{r}_s^C|} \right) \tag{B.6}$$

Equation (B.4) becomes

$$\frac{\partial \mathbf{D}}{\partial t} = \epsilon_0 \frac{\partial \mathbf{E}}{\partial t} = \frac{1}{4\pi} \nabla \int_V \nabla \cdot \frac{\mathbf{J}^s}{|\mathbf{r} - \mathbf{r}_s^C|} dv_s \tag{B.7}$$

Using the curl of curl identity

$$\nabla \times (\nabla \times \mathbf{A}) = \nabla(\nabla \cdot \mathbf{A}) - \nabla^2 \mathbf{A} \tag{B.8}$$

and the fact that

$$\nabla^2 \left(\frac{1}{|\mathbf{r} - \mathbf{r}_s|} \right) = -4\pi \delta(\mathbf{r} - \mathbf{r}_s) \tag{B.9}$$

we conclude, from Equations (B.2) and (B.7), that the magnetic field described in Equation (38) for the capacitor's electrodes satisfies the time-dependent Ampère-Maxwell law

$$\nabla \times \mathbf{B} = \mu_0 \left(\mathbf{J}^s + \frac{\partial \mathbf{D}}{\partial t} \right) = \mu_0 \left(\mathbf{J}^s + \mathbf{J}^D \right) \tag{B.10}$$

This completes the proof that the magnetic field derived satisfies the Ampère-Maxwell law.

References

[1] D. J. Griffiths, Introduction to electrodynamics (2005).

[2] R. P. Feynman, R. B. Leighton, M. Sands, The Feynman Lectures on Physics, Vol. 2, Addison-Wesley, 1964.

[3] A. Mohammadpour, Net force in the absence of external forces in systems with retardation: Emphasis in electromagnetism, working paper or preprint (Feb. 2024).

[4] J. C. Maxwell, Viii. a dynamical theory of the electromagnetic field, Philosophical transactions of the Royal Society of London (155) (1865) 459–512.

[5] C. T. Sebens, Forces on fields, Studies in History and Philosophy of Science Part B: Studies in History and Philosophy of Modern Physics 63 (2018) 1–11.

[6] A. Yaghjian, Reflections on maxwell's treatise, Progress In Electromagnetics Research 149 (2014) 217–249.

[7] J. C. Maxwell, A treatise on electricity and magnetism, Vol. 1, Oxford: Clarendon Press, 1873.

[8] Wikipedia contributors, Lorentz force — Wikipedia, The Free Encyclopedia, [Online; accessed 24-June-2024] (2023).
URL `https://en.wikipedia.org/wiki/Lorentz_force`

[9] D. S. Charrier, Micronewton electromagnetic thruster, Applied Physics Letters 101 (3) (2012).

[10] M. Tuval, A. Yahalom, Newton's third law in the framework of special relativity, The European Physical Journal Plus 129 (2014) 1–8.

[11] K. T. McDonald, Tuval's electromagnetic spaceship.

[12] T. Lafleur, Comment on "micronewton electromagnetic thruster"[appl. phys. lett. 101, 034104 (2012)], Applied Physics Letters 105 (14) (2014).

[13] D. Brady, H. White, P. March, J. Lawrence, F. Davies, Anomalous thrust production from an rf test device measured on a low-thrust torsion pendulum, in: 50th AIAA/ASME/SAE/ASEE Joint Propulsion Conference, 2014, p. 4029.

[14] H. White, P. March, J. Lawrence, J. Vera, A. Sylvester, D. Brady, P. Bailey, Measurement of impulsive thrust from a closed radio-frequency cavity in vacuum, Journal of Propulsion and Power 33 (4) (2017) 830–841.

[15] Y. Raitses, N. Fisch, Parametric investigations of a nonconventional hall thruster, Physics of Plasmas 8 (5) (2001) 2579–2586.

[16] J. Vaudolon, S. Mazouffre, C. Hénaux, D. Harribey, A. Rossi, Optimization of a wall-less hall thruster, Applied Physics Letters 107 (17) (2015).

[17] D. Rafalskyi, J. M. Martínez, L. Habl, E. Zorzoli Rossi, P. Proynov, A. Boré, T. Baret, A. Poyet, T. Lafleur, S. Dudin, et al., In-orbit demonstration of an iodine electric propulsion system, Nature 599 (7885) (2021) 411–415.

[18] K. Takahashi, Thirty percent conversion efficiency from radiofrequency power to thrust energy in a magnetic nozzle plasma thruster, Scientific reports 12 (1) (2022) 18618.

[19] C. Russell, C. Raymond, The dawn mission to minor planets 4 vesta and 1 ceres, Springer Science & Business Media, 2012.

[20] A. N. Aurigema, C. R. Buhler IV, System and method for generating forces using asymmetrical electrostatic pressure, uS Patent 11,511,891 (Nov. 29 2022).

[21] O. D. Jefimenko, Causality, electromagnetic induction, and gravitation: a different approach to the theory of electromagnetic and gravitational fields, Princeton University Press, 2000.

[22] T. B. Bahder, C. Fazi, Force on an asymmetric capacitor, arXiv preprint physics/0211001 (2002).

[23] A. A. Martins, M. J. Pinheiro, On the propulsive force developed by asymmetric capacitors in a vacuum, Physics Procedia 20 (2011) 112–119.

[24] S. Coleman, J. Van Vleck, Origin of" hidden momentum forces" on magnets, Physical Review 171 (5) (1968) 1370.

[25] T. Taylor, Electrodynamic paradox and the center-of-mass principle, Physical Review 137 (2B) (1965) B467.

[26] M. Calkin, Linear momentum of the source of a static electromagnetic field, American Journal of Physics 39 (5) (1971) 513–516.

[27] Y. Du, P. Xia, L. Xiao, Calculating magnetic force of permanent magnet using maxwell stress method, IEEE transactions on applied superconductivity 10 (1) (2000) 1392–1394.

[28] C. Luo, K. Zhang, J. Duan, Y. Jing, Study of permanent magnet electrodynamic suspension system with a novel halbach array, Journal of Electrical Engineering & Technology 15 (2020) 969–977.

[29] M. J. Pinheiro, On newton's third law and its symmetry-breaking effects, Physica Scripta 84 (5) (2011) 055004.

[30] T. Hyodo, Maxwell's displacement current and the magnetic field between capacitor electrodes, European Journal of Physics 43 (6) (2022) 065202.

[31] NASA, Voyager 1 mission overview, accessed: 2024-04-17 (2024).
URL https://science.nasa.gov/mission/voyager/voyager-1/